2022

ADCP Observations of Currents and Suspended Sediment in the Macrotidal Gulf of Martaban, Myanmar

Courtney K. Harris

Jacob T. Wacht

Matthew J. Fair

Jessica M. Cote

frontiers | Frontiers in Earth Science

ORIGINAL RESEARCH
published: 25 April 2022
doi: 10.3389/feart.2022.820326

ADCP Observations of Currents and Suspended Sediment in the Macrotidal Gulf of Martaban, Myanmar

Courtney K. Harris[1]*, *Jacob T. Wacht*[2], *Matthew J. Fair*[1] and *Jessica M. Côté*[3]

[1]*Virginia Institute of Marine Science, William & Mary, Gloucester Point, VA, United States,* [2]*William and Mary, Williamsburg, VA, United States,* [3]*Blue Coast Engineering, Seattle, WA, United States*

The Ayeyarwady and Thanlwin Rivers, which drain Myanmar, together form one of the largest point sources of freshwater and sediment to the global ocean. Combined, these rivers annually deliver an estimated 485 Mt of sediment to the northern Andaman Sea. This sediment contributes to a perennially muddy zone within the macro-tidal Gulf of Martaban, but little is known about the processes that dominate dispersal and trapping of sediment there, as very few water column observations are available. A research cruise in December 2017 provided a rare opportunity to obtain Acoustic Doppler Current Profiler (ADCP) data along transects from the Gulf of Martaban and adjacent continental shelf. Two transects were obtained from the outer portion of the Gulf of Martaban in water depths that ranged from about 20–35 m. These showed very fast currents, especially during flood tide conditions, exceeding 1.5 m/s. The backscatter record from the ADCP indicated asymmetries in distribution of suspended sediment during the ebb versus flood phase of the tide. During ebb tidal conditions, the backscatter record indicated that sediment was transported in either a surface advected layer, or fairly well-mixed throughout the water column. In contrast, during flood tidal conditions, sediment was confined to the bottom boundary layer, even though the velocities were faster during flood than the ebb conditions. The vertical structure of the currents during flood tide conditions indicated the presence of sediment–induced stratification because currents within the near-bed turbid layers were relatively slow, but speeds increased markedly above these layers. This albeit limited dataset provides an exciting glimpse into the dynamics of sediment transport within the muddy, macrotidal Gulf of Martaban, and implies the importance of tidal straining and bottom nepheloid layer formation there.

Keywords: Gulf of Martaban, tidal currents, suspended sediment, macrotidal estuary, ADCP

Edited by:
Daniel R. Parsons,
University of Hull, United Kingdom

Reviewed by:
Kyungsik Choi,
Seoul National University, South Korea
Anabela Oliveira,
Instituto Hidrográfico, Portugal

***Correspondence:**
Courtney K. Harris
ckharris@vims.edu

Specialty section:
This article was submitted to Marine Geoscience, a section of the journal Frontiers in Earth Science

Received: *22 November 2021*
Accepted: *15 March 2022*
Published: *25 April 2022*

Citation:
Harris CK, Wacht JT, Fair MJ and Côté JM (2022) ADCP Observations of Currents and Suspended Sediment in the Macrotidal Gulf of Martaban, Myanmar. Front. Earth Sci. 10:820326. doi: 10.3389/feart.2022.820326

1 INTRODUCTION

Riverine discharge accounts for the majority of sediment input to the ocean, with the largest ~25 rivers accounting for 40% of this sediment (see Milliman and Meade, 1983; Meade, 1996; McKee et al., 2004). Once delivered to oceanic environments, a number of transport processes operate on, and transform sediment and associated nutrients such as organic carbon, before their eventual deposition and burial (McKee et al., 2004). Large Asian rivers draining the Tibetan Plateau are especially significant and account for 25% of global sediment delivery to marginal seas (Kuehl et al., 2020). The third–largest contributor from the Tibetan Planteau is

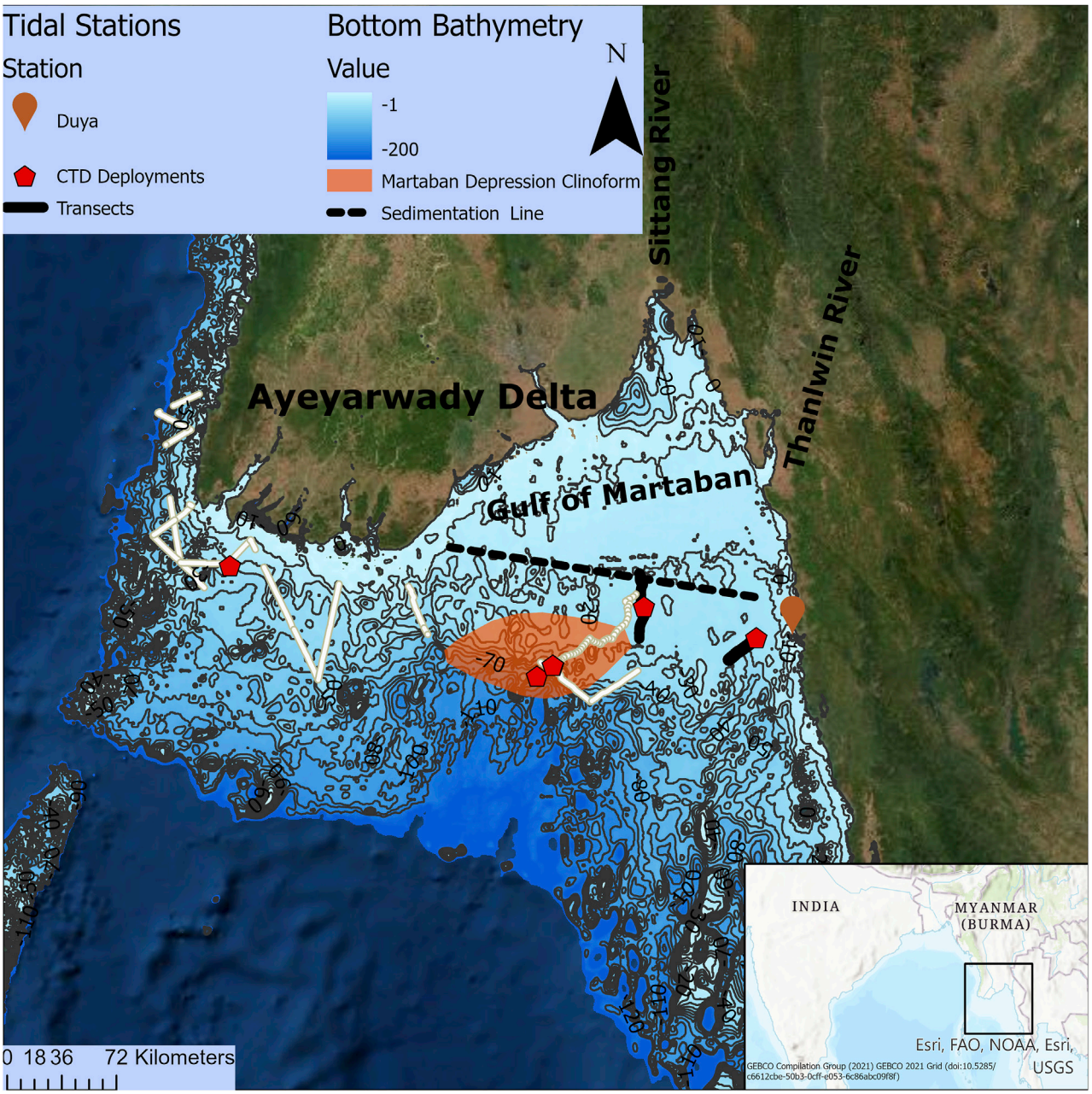

FIGURE 1 | Map of study area in the northern Andaman Sea (see inset for location within Indian Ocean). Black and white lines show locations of all ADCP transects. This manuscript focused on the eastern-most ADCP Transects #5 and #21, shown as black lines. Red markers show locations of CTD-Tu samples. Orange marker shows location of Duya, Myanmar. The dotted black line demarcates areas identified as the mud blanket to the north; and a zone of accumulation to the south (Flynn et al., in press). The orange area in the zone of accumulation represents the location of the Martaban Depresssion Clinoform (Kuehl et al., 2019; Liu et al., 2020).

the combined Ayeyarwady and Thanlwin Rivers (Kuehl et al., 2020). Its combined freshwater discharge is estimated at 528 km^3/year, and sediment discharge at approximately 485 MT per year (Baronas et al., 2020). Additionally, these rivers annually output 5.7–8.8 MT of organic carbon to the coastal ocean, globally ranking second behind the Amazon River (Bird et al., 2008). The Ayeryarwady and Thanlwin Rivers are also relatively unaltered by damming, and as such have been identified as the last non-Arctic long rivers in Asia that remain free flowing (Grill et al., 2019).

Located between the Bay of Bengal and Andaman Sea, the coastal ocean offshore of the Ayeyarwady delta includes a deltaic ramp directly south of the delta; and a shallow but expansive embayment to the east, called the Gulf of Martaban (**Figure 1**). The funnel–shaped Gulf of Martaban is macrotidal, with semi-diurnal tides and a strong spring/neap cycle. Tidal energy

increases toward the eastern side of the Gulf of Martaban, where tidal ranges can exceed 7 m, and tidal current speeds reach 3 m/s (Ramaswamy et al., 2004; Rao et al., 2005). The combination of the influx of riverine muds with strong tidal energy is likely the reason that the Gulf of Martaban exhibits one of the largest perennially muddy coastal areas in the world, covering 45,000 km^2 during spring tides (Ramaswamy et al., 2004). Additionally, the Gulf of Martaban has been identified as one of the most productive areas within the Bay of Bengal; the nutrients delivered by rivers here seem to play a critical role in supporting vital fisheries (Hossain et al., 2020).

The Gulf of Martaban receives sediment and freshwater from the Ayeyarwady River, the Thanlwin River, and the smaller Sittang River; their combined sediment discharge accounts for about 600 MT of sediment potentially input to the Gulf each year (Kuehl et al., 2020). The smallest of these, the Sittang River discharges an estimated 50 MT of sediment annually (Milliman and Farnsworth, 2013). Previous studies have indicated that flows and sediment transport in tidal flats within the Sittang estuary tend to be dominated by the flood tide, but that the morphology may be heavily influenced by ebbing flows during high discharges in the rainy season (Choi et al., 2020). Similarly, *in situ* observations of three distributaries that drain the Ayeyarwady Delta showed these to be exporters of sediment during the rainy season, while during low flow conditions the distributaries may retain sediment delivered from offshore (Glover et al., 2021). While these studies showed that sediment delivery to the Gulf of Martaban responds to spatial, seasonal, and interannual variability; studies have yet to directly link the fluvial sediment sources to the depositional record offshore.

Previous studies have mapped seabed sediment texture within the Gulf (Rao et al., 2005) which has been characterized as a "mud blanket" (Hanebuth et al., 2015). Recently, however, analysis of sediment cores and CHIRP seismic data have provided insight into the depositional environment in this area. The seabed within the shallow Gulf of Martaban contains a thick mixed layer (0.25–1.2 m thick) which is evidence of intense resuspension, but exhibits relatively low accumulation rates (Kuehl et al., 2019). It has been characterized as a "fluid mud reactor" (i.e., Aller, 1998), because the frequent resuspension and apparent trapping within the Gulf likely impact geochemical cycling of organic matter there (Kuehl et al., 2019; Flynn et al., in press). Accumulation rates generally increase offshore in the Gulf of Martaban, and Flynn et al. (in press) note a general transition from the mud blanket to a zone of accumulation at about the mouth of the Gulf (**Figure 1**).

Offshore of the Gulf of Martaban a clinoform depocenter has developed spanning water depths from ~40–130 m (Kuehl et al., 2019; Liu et al., 2020). Termed the Martaban Depression Clinoform (**Figure 1**), this depocenter has been active over the Holocene (Liu et al., 2020); and currently accumulates approximately 6–8 cm/year (Flynn et al., in press; Kuehl et al., 2020). This feature appears to trap a significant fraction of the Ayeryarwady/Thanlwin River discharge of sediment and organic matter (Kuehl et al., 2019; Flynn et al., in press). However, the transport mechanisms that carry material from fluvial sources to the clinoform; and the residence time of material within the mud blanket/fluid mud reactor of the Gulf of Martaban are poorly constrained and limited by our lack of observations from the site.

The oceanographic and coastal dynamics in this region are influenced by tides and seasonal monsoons (Rodolfo, 1969; Ramaswamy and Rao, 2014). From the months May to September the region experiences Southwest (SW) monsoon conditions, dominated by strong winds from the southwest. During the months December through February, the area experiences Northeast (NE) monsoons with moderately strong winds typically from the NE (Ramaswamy and Rao, 2014).

Seasonal fluctuations in circulation have been argued to produce a bi-directional transport pathway; wherein fine-grained sediment would be imported into the Gulf of Martaban during the energetic SW monsoon, but exported westward during NE monsoon conditions (Anthony et al., 2019; Kuehl et al., 2019; Liu et al., 2020; Glover et al., 2021). Generally, historical data from this location and satellite observations have been used to characterize surface currents (Rodolfo, 1975; Rao et al., 2005), but the directions of the near-bed flows that dictate sediment movement and fate remain unclear. Additionally, CTD-Tu (Currents/Temperature/Depth/Turbidity) casts obtained in December 2017 indicated the presence of fluid mud in the bottom meters of the water column within the Gulf of Martaban (Kuehl et al., 2019). The presence of these fluid mud layers implies that the surface currents that have been characterized may be very different from near-bed currents that control sediment movement. Little is known about the near-bed processes and circulation that are responsible for maintaining the turbidity within the Gulf of Martaban, or for delivering material to offshore depocenters.

Direct observations of suspended concentrations for the Gulf of Martaban are limited to an april/May 2002 study that used filtered water samples to characterize sediment concentrations as being in the 100s of mg/L, and composed of terrigenous silty clays (Ramaswamy et al., 2004). Satellite data have been used to infer spatial patterns and have shown that turbidity in the Gulf of Martaban is especially responsive to the spring/neap cycle, with the extent of the turbid zone being largest during spring tides (Ramaswamy et al., 2004). Compilations of satellite images have also indicated a seasonal signal to the surface turbidity, with the turbid zone covering the largest expanse during the NE monsoon season of December–February (Matamin et al., 2015). Analysis of satellite data has indicated that seasonal suspended sediment concentrations are highest in December, when monthly averaged surface concentrations were estimated to exceed 200 mg/L throughout the Gulf of Martaban (Anthony et al., 2019).

In summary, the Gulf of Martaban has a global significance in terms of sediment and organic carbon transfer from land to ocean, and in basin-scale fisheries productivity. In spite of this, very little has been observed regarding estuarine hydrodynamics or suspended sediment transport within the Gulf. At present we lack data to constrain the sediment transport mechanisms that carry material from fluvial sources, through their residence in the muddy Gulf of Martaban, to their ultimate deposition in the clinoform depocenter. Observations of currents and turbidity at depth are needed to test numerical and conceptual models of hydrodynamics and sediment transport, and constrain sediment

transport pathways there. This manuscript presents data from two ADCP (Acoustic Doppler Current Profiler) transects that were obtained during December 2017 from the outer Gulf of Martaban.

2 MATERIALS AND METHODS

Within this paper, we provide a unique glimpse at hydrodynamics and sediment dynamics for the Gulf of Martaban, based primarily on water column observations taken during a research cruise.

2.1 Cruise Data

During December 2017 a research cruise was conducted on the vessel the Sea Princess over the Ayeyarwady subaqueous delta and within the Gulf of Martaban (Kuehl et al., 2019; Liu et al., 2020). Though the primary focus of the cruise was to obtain sediment bed samples and map the seafloor, it afforded a rare opportunity to obtain water column data.

2.1.1 ADCP Data

During the cruise, which surveyed over 1500-km in the northern Andaman Sea and Bay of Bengal, an ADCP was mounted from the boat, facing vertically downward to record current velocities and acoustic backscatter within the water column. Though it was not calibrated, the backscatter intensity of the ADCP acts as a proxy for the relative magnitudes and vertical distribution of suspended sediment concentrations (e.g., Holdaway et al., 1999). During this cruise, over fifteen ADCP transects were recorded covering a large geographic portion of the coastal Ayeyarwady delta and Gulf of Martaban (**Figure 1**). The TRDI (Teledyne RD Instruments) 600 kHz ADCP was configured in mode 12 and recorded measurements from 255 vertical bins each with a thickness of 33 cm for a maximum coverage of 84 m water depth. Bottom tracking that assumed the presence of a static seafloor was used to adjust current velocities to account for the boat's speed relative to the sea floor. Of these ADCP transects, six were chosen for initial analysis. Data from transects located south and west of the Ayeyarwady Delta showed a general westward direction to currents, consistent with seasonal patterns of circulation that have been published (Rodolfo, 1975; Ramaswamy and Rao, 2014). However, because the sampling period was short relative to the expected variability of non-tidal currents, this paper is limited to analyzing the ADCP data from within the tidally dominated area.

This paper focuses on two transects taken in the outer Gulf of Martaban. Transects #5 and #21 (see **Figure 1**) provided insight into the tidal control on sediment dispersal in the outer Gulf of Martaban. These two transects covered water depths that ranged from about 20–35 m. Transect #5 was located along the eastern side of the outer Gulf, while Transect #21 was located in the central area of the outer Gulf (**Figure 1**). In discussing the ADCP data, locations will be referenced with respect to distance along the transects.

Suspended sediment concentrations cannot be directly inferred from the backscatter data, because they were not calibrated. Sediment cores taken prior to both transects showed variations in grain size, indicating that sand fraction varied from ~3 to ~30% within the area sampled by these transects (data from Kuehl et al., 2019), while suspended material was previously characterized as silty clay (Ramaswamy et al., 2004). Seabed organic content in this area was fairly uniform at about 0.6–0.7% (Flynn et al., in press). Water column samples were not obtained with which to characterize suspended grain sizes or concentrations, but the ADCP backscatter remains useful for characterizing the vertical distribution of, and relative concentrations of suspended material.

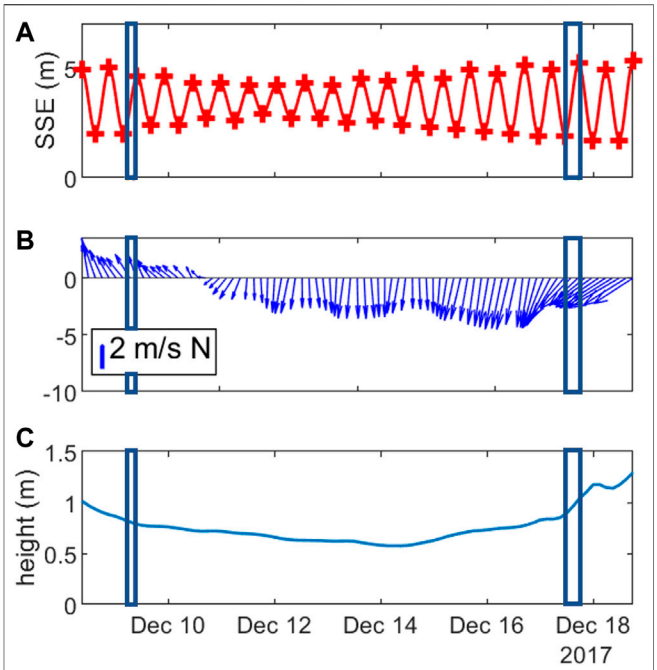

FIGURE 2 | Timeseries of oceanographic and meteorological conditions during the December 2017 research cruise. Transects #5 and #21 were obtained during the times marked. **(A)** Times of high and low tidal elevation for Duya, Myanmar (Egbert and Erofeeva, 2002). **(B)** Wind vectors and **(C)** Wave heights from GFS (Environmental Modeling Center, 2003). Wind vectors show direction toward which the modeled wind blew.

For each transect, a principal axis for the current velocity was identified using a Principal Component Analysis (PCA). The principal axes for both transects were generally oriented in a northeast/southwest direction, and the majority of the variability in the currents was along the major axes. This manuscript reports velocities components that are rotated to be along and perpendicular to the major axis of the currents, which we term the local "along Gulf" direction.

2.1.2 CTD-Tu Data

While on the cruise, several CTD-Tu (Conductivity, Temperature, Depth, and Turbidity) profiles were taken when the ship was anchored. Specifically, the CTD-Tu (RBR XRX-620) package was manually deployed, sampling at 6 Hz during descent through the water column at a rate of ~20 cm s−1. An OBS was mounted on the CTD and its voltage readings indicate relative turbidity, but were not calibrated to provide suspended sediment concentration. These were analyzed previously and shown to provide evidence that fluid muds

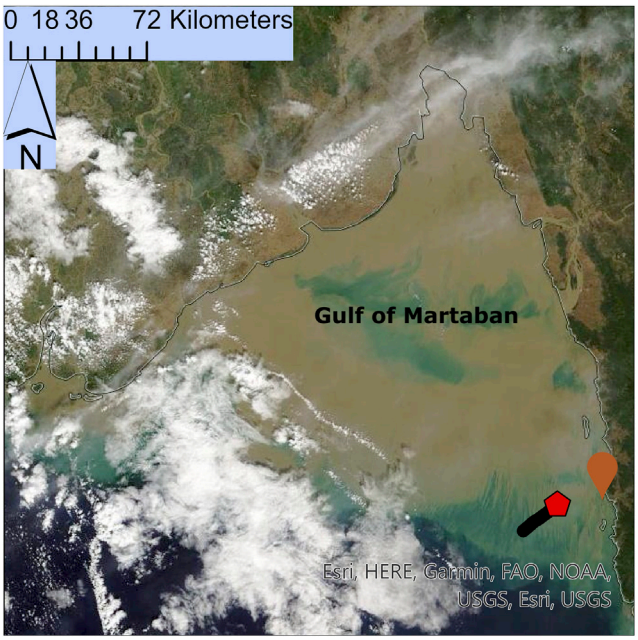

FIGURE 3 | Satellite image taken within a day of ADCP Transect #5. Location of transect (black line) and CTD-Tu (red circle) shown. Duya, Myanmar shown as orange marker. Image from NASA Worldview.

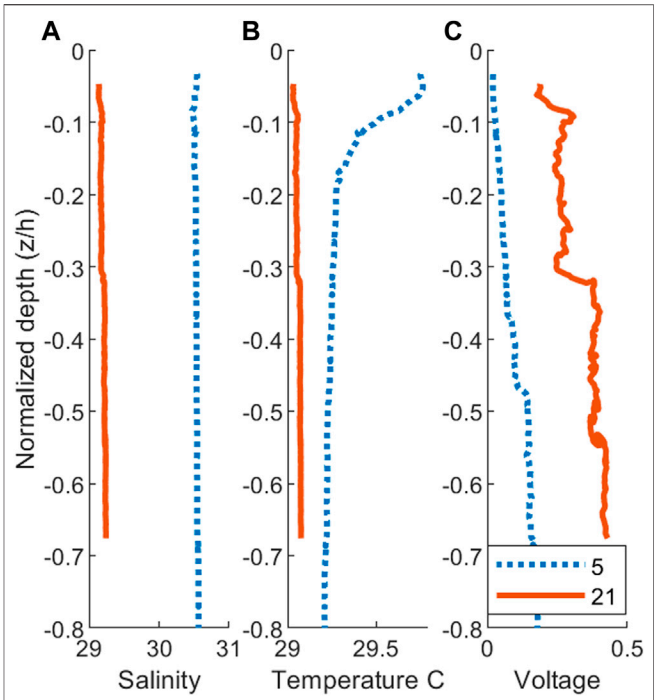

FIGURE 4 | Vertical profiles of **(A)** Salinity, **(B)** Temperature, and **(C)** Voltage from CTD-Tu. Vertical axes represent the normalized depth (z/total water depth). CTD-Tu profiles taken directly before Transect #5 (red lines) and during Transect #21 (blue dashed lines).

exist within the Gulf of Martaban, having vertical thicknesses of a few meters (Kuehl et al., 2019). Two of these CTD-Tu profiles, obtained nearly concurrently with ADCP Transects #5 and #21, are used within this manuscript to characterize water column structure to as a complement to the ADCP data.

2.2 Ancillary Data

Observations of oceanographic and meteorological data are largely unavailable for the Gulf of Martaban. Therefore, data from global numerical models provided useful information for placing the ADCP data in the context of the oceanographic and meteorological conditions present during the cruise. Data from a global tidal model (Egbert and Erofeeva, 2002) for the location of Duva, Myanmar (see **Figure 1**) allowed us to characterize the tidal conditions at the time of ADCP deployment (**Figure 2A**). Because local measurements of winds and waves were not available for the Gulf of Martaban, we used a global numerical model, the Global Forecast System (GFS (Environmental Modeling Center, 2003)) to classify the meteorological conditions during the cruise (**Figures 2B–C**). Additionally, satellite imagery from NASA Worldview Application (2021) allowed us to put the ADCP transect observations into the larger spatial context.

3 RESULTS

This section provides the observed current velocities and ADCP backscatter for two transects from the outer Gulf of Martaban recorded in December 2017. Both of these ADCP transects were initiated near the end of ebb tide; continuing through low tide and the transition into flood tide conditions (**Figure 2A**). Output from the global GFS model indicated that conditions during the cruise were rather calm, with wave heights estimated to be ~1 m (**Figure 2C**). Wind speeds were estimated at < 5 m/s, and the GFS model indicated that winds turned from being from the northwest early in the cruise, and then were primarily from the northeast (**Figure 2B**).

3.1 Eastern Gulf of Martaban: Transect #5

Transect #5 was recorded on 9 December 2017 beginning at 05:34 UTC and finishing at 08:40 UTC. The transect covered about 22 km on the eastern side of the Gulf of Martaban, with the boat traveling westward toward the middle of the Gulf of Martaban (**Figure 3**). Water depths along the transect spanned from about 25 to 35 m, with the shallowest region sampled earliest in the transect. Based on water level at the closest tidal station to the transect (Duya), tidal conditions during the 3-h transit spanned from the end of ebb tide, through slack, to flood tide (**Figure 2A**). Sediment cores were taken immediately prior to, and following the ADCP transect. These data indicate that there was little change in organic content (~0.6%); though seabed texture changed from muddy near the start of the transect, to mixed sediments (sand, silt, and clay) at the deeper end of the transect (Kuehl et al., 2019; Flynn et al., in press). The satellite imagery from the day prior to the ADCP deployment shows the sampling location to be within the fringe of the extent of the turbid waters of the Gulf of Martaban (**Figure 3**).

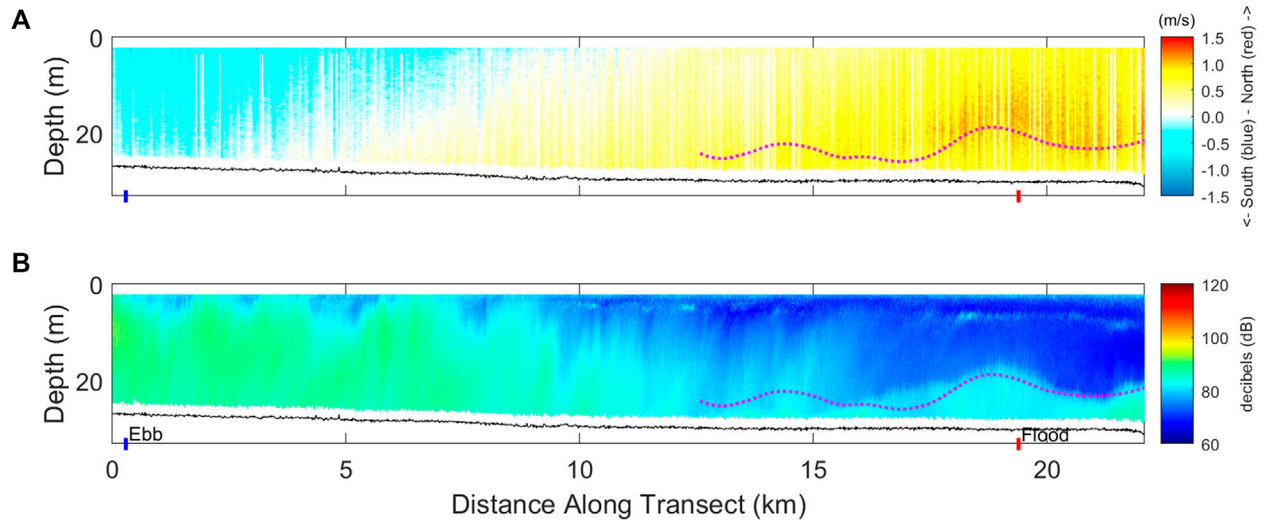

FIGURE 5 | Data observed along Transect #5. The distance traveled along the transect is shown on the horizontal axis, and water depth along the vertical axes. Depth in the water column was estimated after accounting for the approximate submerged depth of the ADCP sensor. The black line represents approximate location of the seafloor. **(A)**: water speed (m/s) in direction of primary axis, which was 9.4° clockwise from North. Blue colors indicate southward flow; red indicates northward flow. **(B)**: backscatter intensity (a measure of the return energy in decibels [dB]). The data was filtered using the Winriver II software and then a triangular smoothing filter was applied. The white vertical bars in **(A)** represent data that was removed because either the GPS or bottom tracking was deemed unreliable. The blue and red tick marks on the *x*-axis represent the position along the transect of ebb and flood, respectively, shown in **Figure 8**. The dotted lines during flood tide (~12–25 km) represent the approximate thickness of the near-bed turbid layer, as described in **Section 4.1**.

Additionally, a CTD-Tu was obtained immediately before Transect #5. This showed that the water column was well-mixed, with a thin (~few meters) surface layer that had slightly depressed salinity and increased temperature (**Figures 4A,B**). The voltage for the OBS (Optical Backscatter Sensor) provides a measure of the vertical structure of water column turbidity. It showed relatively low backscatter (~0.3 V) and indicated that the suspended sediment was well mixed at this time (**Figure 4C**). For comparison, OBS readings reached 4 V at other locations and times during this cruise (Kuehl et al., 2019).

The Principal Component Analysis (PCA) performed on the velocity data from Transect #5 showed that the principal axis of the velocities was directed 9.4° clockwise from North, aligned generally in "along Gulf" and "across Gulf" directions. The currents were strongly oscillatory, with components along the principal axis containing most (93%) of the variability in the currents. The component of the currents perpendicular to the principal axis had much smaller magnitudes (0.1 m/s), compared to velocity components that exceeded 1 m/s along the principal axis.

Considering the ADCP data in terms of the spatial variations along the 22-km transect, conditions observed over the shallower portion of the transect (0–7 km on **Figure 5A**) had a well–mixed water column with moderate current velocities. The backscatter in this portion of the transect indicated that suspended sediment was mixed throughout the water column, except for surface layers that had small backscatter (0–7 km on **Figure 5B**). This was consistent with the CTD-Tu record that showed little evidence of stratification or isolated layers of turbidity. When the boat traveled into deeper water away from the coast (17–23 km on **Figure 5**), current velocities accelerated, and the backscatter indicated that a near-bed turbid layer developed.

The changes observed along the transect correspond to tidal forcing. Considering the temporal changes in the current speed and direction (**Figure 5A**), the ADCP data show the transition from ebb to flood conditions. Initially, during the first ~5 km of the transect, which coincided with the end of ebb tide, there were moderate speeds of about 0.5 m/s that flowed southward (**Figure 5A**). Next, the speeds slowed to zero during slack water at low tide from ~5–10 km along the transect. Then, as the tide turned to flood, the current direction shifted northward and speeds exceeded 1 m/s from ~17 km to the end of the transect (**Figure 5A**).

Similarly, the backscatter intensity showed a strong relationship to the tides, indicating tidal forcing of suspended sediment. Initially, during ebb (from 0 to 5 km along the transect) there was usually a high return at all depths suggesting suspended sediment was well mixed throughout the water column (**Figure 5B**). At some times, there was evidence of clear surface plumes in the upper 3–5 m of the water, for example at 1, 3 and 5 km along the transect (**Figure 5B**). As the water speeds slowed during slack water at low tide, the upper water column cleared (at about 6–12 km in **Figure 5B**). As tidal currents turned to flood tide and accelerated, a two-layer system developed (20 km to the end of the transect, **Figure 5B**). There was evidence of suspended sediment in the bottom-most 5 m of the water column, above which the backscatter intensity showed a sharp decrease indicating the presence of a near-bed turbid layer overlain by clearer water. The current velocity also showed speeds were slow within the turbid layer but reached very fast speeds (~1.5 m/s) directly above the turbid layer (**Figure 5**).

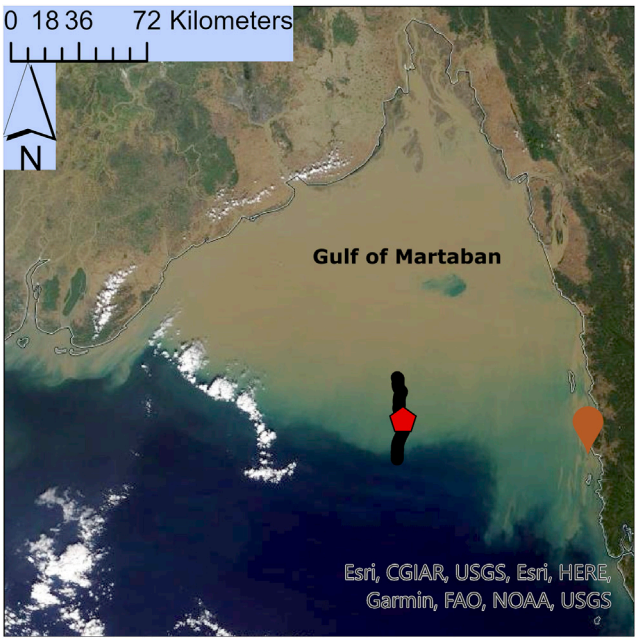

FIGURE 6 | Satellite image taken on the same day that Transect #21 was sampled. Location of transect (black line) and CTD-tu (red mark) shown. Duya, Myanmar shown as orange mark. Image from NASA Worldview.

3.2 Central Gulf of Martaban: Transect #21

Transect #21 was collected in two sections in the outer portion of the central Gulf of Martaban, with a gap of about 10-min between the two collection periods. Sampling began on December 17, at 11:39 UTC, and concluded on 17:26 UTC (**Figure 6**). The data from these two sections covered about 39 km, and were obtained over about 6 h. It sampled water depths that ranged from 20–30 m with the boat traveling southward. Additionally, a CTD-Tu was obtained during the gap in the ADCP collection. Similar to Transect #5, during the time when Transect #21 was sampled, the tides went from ebbing, through low tide at slack water, and then reached flood tide (**Figure 2**). A sediment core taken adjacent to Transect #21 showed that the seabed was about 20% sand and 80% mud; with an organic content of about 0.6% (Kuehl et al., 2019; Flynn et al., in press).

Principal Components Analysis (PCA) of the velocity data from Transect #21 showed that the principal axis of the velocities was directed 20.5° clockwise from North; roughly aligned with "along Gulf' and "across Gulf" directions. The currents at this location were strongly oscillatory, with components along the principal axis containing most (92%) of the variability in the currents. The velocity components perpendicular to the principal axis were an order of magnitude smaller (0.12 m/s) than the velocity components along the principal axis, which reached magnitudes of 1.5 m/s.

Three distinct portions of Transect #21 are evident. At the most shoreward portion of the transect (0–7 km), velocities were high (~1 m/s) and southward, and the backscatter indicated the presence of a surface turbid plume (**Figure 7**). In the next region (~7–17 km), current velocities slowed, and the turbid water was found at increasing water depths (**Figure 7**). The CTD-Tu taken in the middle of Transect 21 was located around 20 km (**Figure 4**). It showed a fairly well-mixed water column with relatively low voltage by the OBS (~0.5 V), indicating low sediment concentrations compared to other locations that were sampled during the cruise (i.e. Kuehl et al., 2019). In the more seaward portion of the transect (~25–39 km), the backscatter indicated the presence of a near-bed turbid layer, while turbidity in the upper water column was reduced (**Figure 7B**). At this point in the transect (~25–39 km), the northward directed current velocities reached high speeds (~1.5 m/s; **Figure 7A**).

The temporal changes in the current speed and direction along Transect #21 correspond to tidal forcing and show the transition from ebb to flood conditions (**Figure 7A**). The first ~10 km of the transect coincided with the timing of the ebb tide. The highest observed currents during the ebb were about 1 m/s, flowing offshore (**Figure 7A**). Next, the speeds fell to zero during slack water at low tide from ~12–17 km along the transect. Then, as the tide turned to flood, the current direction shifted northward, and speeds exceeded 1.2 m/s from ~25 km to the end of the transect (**Figure 7A**).

The backscatter record indicated that the vertical distribution of suspended sediment also responded to tidal forcing. At the beginning of the transect (0–8 km), the current was ebbing, and there were two distinct backscatter layers (**Figure 7B**). At this time, the surface waters showed much more backscatter than the lower water column, indicating that the ebb tide was exporting muddy water in the surface layer from the Gulf of Martaban. During slack tide, from 8–18 km along the transect, sediment appeared to settle as the turbid layer shifted from surface waters toward the mid-water column (**Figure 7B**). Then, flood tide commenced, and current speeds increased (20–35 km along the transect), and a near-bed turbid layer appeared in the bottom few meters of the water column (**Figure 7B**). This suspended layer experienced northward flux in the relatively thin near-bed bottom layer. Sediment concentrations during the flood tide appeared to be smaller than during the ebb tide, based on comparing the backscatter intensity during these times (**Figure 7B**).

In summary, over the conditions observed for Transect #21, fast currents (>1 m/s) occurred during both ebb and flood tidal conditions. The backscatter indicated more sediment was suspended during the ebb tide than the flood tide, even though observed currents were faster during flood. This was expected since the ebb transports water from the more turbid estuarine waters, carrying it seaward (see **Figure 6**). During the strong flows observed during the flood tidal phase, a two-layer flow developed with a turbid near-bed layer.

4 DISCUSSION

Here, the ADCP data from both transects are synthesized to look for common features during ebb and flood tide conditions, and qualitatively assessed to evaluate net sediment fluxes over the ebb–to–flood tide.

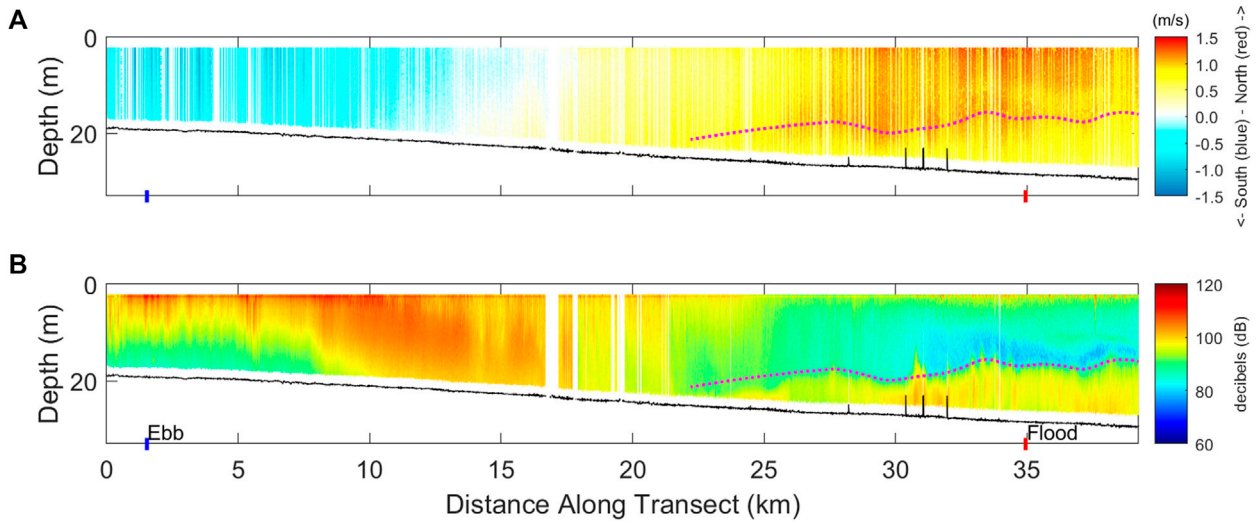

FIGURE 7 | Data observed along Transect #21. The distance traveled along the transect is shown on the horizontal axis, and water depth along the vertical axes. Depth in the water column was estimated after accounting for the approximate submerged depth of the ADCP sensor. The black line represents approximate location of the seafloor. **(A)**: water speed in direction of primary axis is displayed in the colorbar in m/s, which was 20.5 ° clockwise from North. Blue colors indicate flow out of the Gulf, red indicates flow into the Gulf **(B)**: backscatter intensity (a measure of the return energy in decibels [dB]) in the colorbar. High values of backscatter intensity indicate the presence of suspended sediment. The data was filtered using the Winriver II software and then a triangular smoothing filter was applied. The white vertical bars in **(A)** represent data that was removed because either the GPS or bottom tracking was deemed unreliable. The blue and red tick marks on the *x*-axis represent the position along the transect of ebb and flood, respectively, shown in **Figure 8**. The dashed lines during flood tide (~23–40 km) represent the approximate thickness of the near-bed turbid layer, as described in **Section 4.1**.

4.1 Vertical Structure of Ebb vs Flood

Comparing conditions observed at these two transects (e.g., **Figure 4**), the eastern Gulf of Martaban (Transect #5) had higher salinity than the transect from the central Gulf of Martaban (Transect #21). Satellite imagery indicated that the surficial suspended sediment concentrations would be higher in the central region compared to the eastern Gulf of Martaban (**Figure 3**, **Figure 6**), and the ADCP backscatter was consistent with this: showing higher backscatter for Transect #21 than #5 (**Figure 5B**, **Figure 7B**). Additionally, the ADCP transects show that the eastern region had lower current velocities than the central region, at least for the time sampled (**Figure 5A**, **Figure 7A**). Current speeds along both transects reached magnitudes of about 1.5 m/s during flood tide, and for both transects the fastest currents occurred in the mid-water column during flood (**Figure 5A**, **Figure 7A**).

To better visualize the vertical structure of the currents and suspended sediment, profiles for each were taken from Transects #5 and #21 that were representative of ebb and flood conditions (**Figure 8**). These profiles present data that was smoothed by time-averaging the samples for 1-min along the transect, and by applying a 1-m running average in the vertical. For both transects, the profiles for flood tide had faster current velocities than the ebb tide (**Figures 8A,C**). Additionally, the vertical structure for the flood tides showed more shear at both locations than the ebb tide; and the flood tide had a mid-water column peak in speed, whereas the ebb tides showed current speeds to increase toward the surface water (**Figures 8A,C**).

Though currents were faster for these profiles during flood conditions than ebb, the acoustic backscatter were higher during ebb than flood (**Figure 8**). This indicates that concentrations were higher during ebb than flood. The acoustic backscatter from both transects showed that the vertical distribution of suspended sediment differed during ebb tide compared to flood (**Figures 8B,C**). During ebb tide, suspended sediment was fairly well–mixed at Transect #5 (**Figure 8B**), while a surface turbid layer was seen in the central Gulf of Martaban (Transect #21; **Figure 8D**). During flood conditions, however, the acoustic backscatter from both transects indicated the presence of near-bed turbid layers, with high backscatter evident in the bottom 40% of the water column (**Figures 8B,D**).

The backscatter records from both transects were analyzed to look for a sharp vertical gradient in suspended sediment concentrations, i.e., a lutocline. The thickness of the near-bed turbid layer for the flood portions of the transects were identified and are shown as dotted lines in **Figure 5B**, **Figure 7B**. The lutocline was identified as the deepest point for which a threshold backscatter reading was observed. High-frequency variability in the layer thickness was removed by application of a Robust Loess smoothing function. Thus identified, these near-bed layers ranged from about 2–11 m in thickness (dotted lines in **Figure 5B**, **Figure 7B**). Interestingly, the velocity structure of the flood–tidal currents showed a similar behavior to the thickness of the near-bed turbid layer. Velocities within the turbid layer tended to be lower than the velocities immediately above the turbid layer, and the thickness of these turbid layers aligned with the approximate height of the mid-water column peak in speeds (**Figure 5A**, **Figure 7A**).

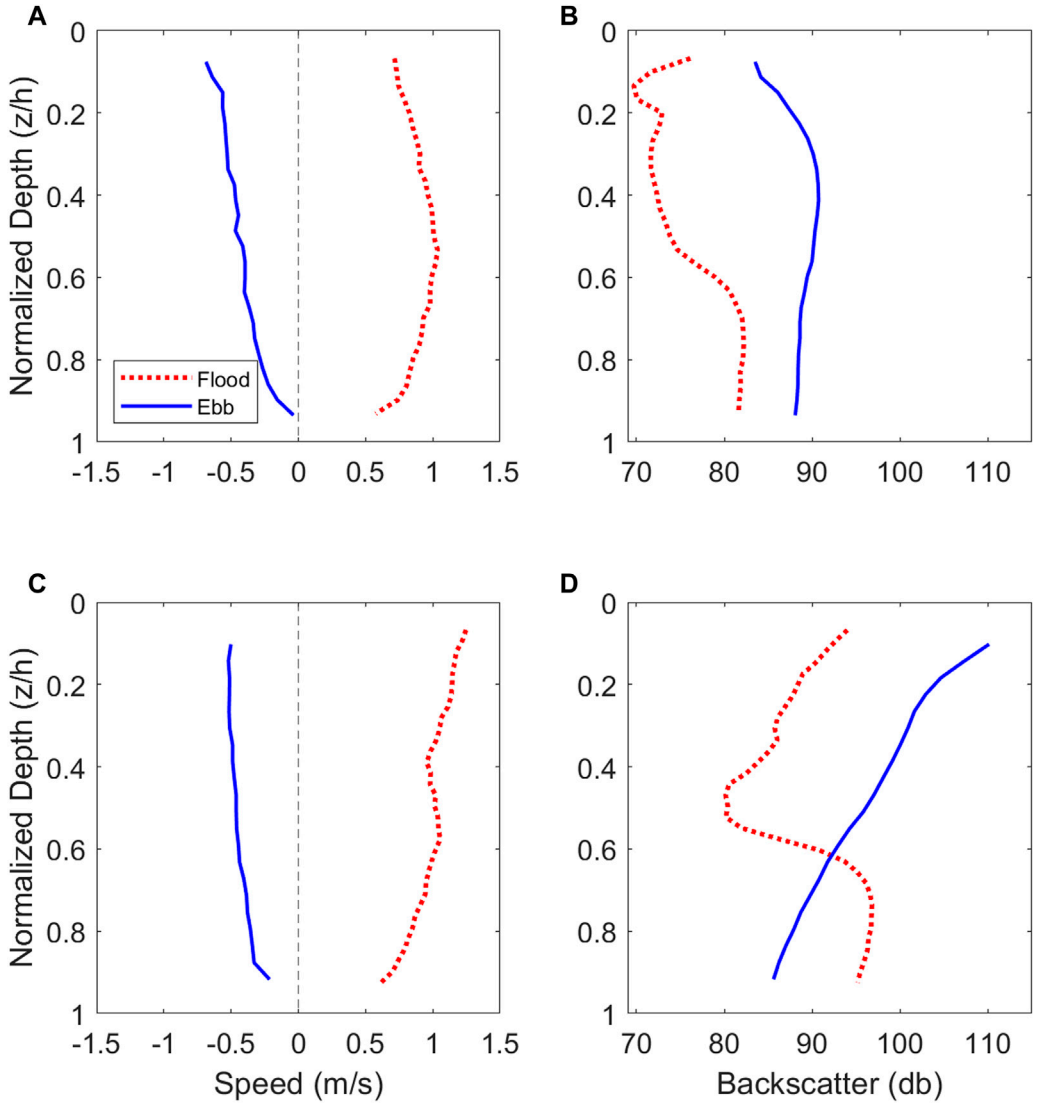

FIGURE 8 | Vertical profiles of velocity and backscatter from Transects #5 and #21 taken during Ebb and Flood conditions. The profiles averaged the measurements for 1-min; and over1-m depth intervals. Panels **(A)** and **(C)** display the velocity components and speed. Panels **(B)** and **(D)** show the backscatter return.

This provides evidence that sediment–induced stratification (Smith and McLean, 1977; Glenn and Grant, 1987) dampened vertical mixing and influenced the vertical structure of the observed currents during flood tide conditions. The reduced velocities within the turbid bottom layer could be attributed to enhanced drag and reduced turbulent mixing due to the increased density gradient in the bottom layers (e.g., Trowbridge and Kineke 1994; Friedrichs et al., 2000).

4.2 Tidal Modulation of Sediment Flux

Because the ADCP backscatter was not calibrated for suspended sediment, and because the transects did not cover a full ebb–to–flood tidal cycle, it is impossible to quantitatively assess sediment fluxes. However, the backscatter and current velocity data indicate that seaward sediment flux was an important component of the net flux for the conditions sampled. The ADCP backscatter was higher during ebb conditions than flood for both transects (**Figures 8B,D**). During flood conditions at both transects, near-bed turbid layers appeared, but they had lower backscatter values than those seen for ebb conditions (**Figures 8B,D**). Additionally, current velocities were depressed in the bottom boundary layer where these turbid layers formed (**Figures 8A,C**). Furthermore the transects were begun during the waning portion of ebb conditions, when velocities were decreasing and therefore likely underestimated the capacity of the ebb tides to transport sediment. Taken together, these indicate that the flood tides would not be very effective at transporting sediment, so that

the ebb tides may contribute a significant part of the net sediment flux.

The ADCP data, made in water depths of ~30 m, contrast somewhat with the observations that have been made in the shallower, tidal-river portions of the sedimentary system. For example, water column observations obtained over a 3-day period on a tidal flat of the Sittang River, saw sediment fluxes were dominated by landward pulses during flood tidal bores (Choi et al., 2020). Geomorphology indicated that over longer-term timescales (seasonal to century), however, ebbing conditions during high discharges (i.e., during the southeast monsoon, or tropical cyclones) were important to maintaining the structures of the Sittang River channels and meander bends (Choi et al., 2020). Water column observations from three distributary channels that spanned the Ayeyarwady Delta similarly showed a seasonal variation in ebb vs flood-tide dominance of sediment flux (Glover et al., 2021). During the rainy season, the three distributary channels showed export of fluvial sediment to the shelf. During the low flow season, however, the eastern-most distributary (the Yangon River estuary) appeared to have sediment fluxes dominated by the flood tide indicating that sediment from the Gulf of Martaban was transported landward in this channel during these conditions (Glover et al., 2021).

These ADCP transects were located in the transition zone between what has been characterized as a "fluid mud reactor" (i.e., Aller 1998) within the shallow Gulf of Martaban and the clinoform depocenter (Kuehl et al., 2019; Liu et al., 2020). Transect #21, in particular, was located at the landward edge of the clinoform (**Figure 1**). The residence time of sediment within the Gulf, and resultant geochemical cycling of organic matter associated with the sediment, depend on the specific transport mechanisms that deliver material from the muddy Gulf of Martaban to the depocenter. Mechanisms that have been suggested for delivering sediment from the turbid Gulf of Martaban to the clinoform include bottom nepheloid layers, seasonal variations in wind-driven currents, storm-driven transport, and tidally modulated fluxes (Ramaswamy et al., 2004; Liu et al., 2020).

Though limited in scope, the data from this study indicate that tidal pumping creates export of sediment during ebb tides that deliver sediment from the Gulf of Martaban to the depocenter. It also implies that tidal straining, whereby stratification effects impact the vertical distribution of momentum and suspended sediment concentration may play a role. Classically, tidal straining has been attributed to variations in density due to salinity (i.e., Simpson et al., 1990), and many estuaries exhibit the straining effect during ebb tides when freshwater is carried over more salty water (e.g., Scully and Friedrichs 2007). In the Gulf of Martaban data, however, the suppression of turbulence appears to occur during flood conditions, when the clearer water from the deep–sea is carried over the muddy water from the Gulf of Martaban. Similar behavior has been observed in the Huanghe Estuary, and attributed to longitudinal variations in suspended sediment availability (Wang and Wang 2010).

The apparent importance of ebb tidal sediment flux for these locations within the Gulf of Martaban provide an interesting contrast to other estuaries that have been classified as flood dominant. To better quantify the sediment residence times within the Gulf of Martaban, and delivery mechanisms from riverine sources to the clinoform depocenter, however, obviously requires consideration of larger spatical scales and longer timescales. Numerical models that couple hydrodynamics and suspended sediment that can reproduce the vertical structure of these ebb and flood conditions may provide insight into the transport mechanisms that carry sediment from the turbid zone to depocenters. Multi-scale numerical models would be needed to place in context the relative contributions of seasonal, tidal, and spatial variations in sediment delivery that have been observed in the tidal rivers of the system (e.g., Choi et al., 2020; Glover et al., 2021), with the larger scale development of the Gulf mud blanket and Martaban Depression clinoform. Additionally, a three-dimensional numerical model could put these limited observations into the larger context of the Gulf of Martaban by accounting for exchanges with the Ayeryarwady delta region, the impact of baroclinic forcings, spring/neap variability, and seasonal variations in winds and wave energy.

5 CONCLUSION

Though limited, this dataset provides rare observations of currents and acoustic backscatter for the outer portion of the central and eastern Gulf of Martaban, one of the world's largest perennially turbid coastal areas. The observations, made in ~20–35 m water depths, indicated that the currents are strongly oscillatory. The primary axes of the currents were directed in generally northeast/southwest direction at both transects. Over the times sampled, surface currents oscillated between 1 m/s seaward (during ebb) to >1.5 m/s landward (during flood), and velocity components were much larger in the along-Gulf directions compared to the across-Gulf directions. Both transects were sampled as ebb tide conditions gave way to slack, and then flood conditions. For the situations that were sampled, the flood velocities exceeded the current speeds observed during ebb conditions. The ADCP backscatter also indicated that the vertical distribution of suspended sediment varied spatially and with the tidal conditions. Acoustic backscatter and satellite imagery indicated larger suspended sediment concentrations in the central Gulf of Martaban than in the eastern Gulf of Martaban. For both transects, the backscatter signal was larger during ebb conditions than flood, even though current velocities were faster during flood. During ebb tidal conditions, suspended sediment appeared vertically well–mixed in the eastern Gulf transect; or formed a surface plume in the central Gulf transect. During slack tide, both transects recorded that the suspended sediment seemed to settle toward the bottom. For both transects as slack gave way to flood tide, fast currents coincided with the appearance of a near-bed turbid area that ranged from 2–11 m in thickness. During flood tide at both transects, the velocity profiles showed mid-water column maximums in current speeds. The upper limit of the thickness of the near-bed turbid layer was similar to the height of the maximums in velocity. This could indicate a feedback

mechanism between the near-bed turbidity and velocity shear, such as suspended–sediment induced stratification that would be expected for conditions of near-bed fluid muds or bottom nepheloid layers. Though it bears more consideration, the data indicate that tidal straining during flood conditions limited the flood-tidal sediment inputs into the Gulf of Martaban, while export of sediment during ebb conditions is an important component of the net sediment balance for the outer Gulf of Martaban. This data indicates that ebb-tidal delivery may be an important mechanism for delivering material from the Gulf of Martaban mud blanket to the Martaban Depression clinoform.

DATA AVAILABILITY STATEMENT

This article uses data from two online repositories. The ADCP datasets can be found in Harris and Wacht (2021). *"Acoustic Doppler Current Profiler (ADCP) data 2017: Ayeyarwady Delta, Myanmar"*. William & Mary. https://doi.org/10.25773/e55p-dd70. The CTD-Tu data was archived in Kuehl and Harris (2020) *"Fate of Ayeyarwady and Thanlwin River sediment: relative importance of oceanographic and tectonic controls - Associated dataset"*. William & Mary. https://doi.org/10.25773/g7zk-sg96.

AUTHOR CONTRIBUTIONS

CH, JW: conceptualization writing-original draft preparation. CH, JW, and JC: ADCP methodology. MF and JW: ancilliary data. CH: supervision and funding acquisition. All: writing-review and editing. All authors have read and agreed to the published version of the manuscript.

FUNDING

This research was supported by the National Science Foundation, USA grant OCE-1737221.

ACKNOWLEDGMENTS

This paper is Contribution No. 4080 of the Virginia Institute of Marine Science, William and Mary. The authors thank Steve Kuehl (VIMS) who acted as chief scientist on the research cruise and commented on earlier presentations of this work; and Danielle Tarpley (VIMS, ACOE) who oversaw the ADCP deployment. Additionally, Paul Liu (NC State University) aided with ADCP deployment, cruise logistics, and project design. We appreciate conversations with Todd Averett and Jeff Nelson (both William and Mary) and Andrea Ogston (U. Washington) that improved the work. The authors express their deepest appreciation to the students and faculty at University of Yangon and Mawlamyine University who supported and participated in the research cruise. We also thank the Captain and crew of the Yangon-based Sea Princess, as this study would not have been possible without their efforts. Finally, we appreciate the helpful and insightful comments of two reviewers, which we feel helped improve the manuscript.

REFERENCES

Aller, R. C. (1998). Mobile Deltaic and Continental Shelf Muds as Suboxic, Fluidized Bed Reactors. *Mar. Chem.* 61 (3-4), 143–155. doi:10.1016/s0304-4203(98)00024-3

Anthony, E. J., Besset, M., Dussouillez, P., Goichot, M., and Loisel, H. (2019). Overview of the Monsoon-Influenced Ayeyarwady River Delta, and Delta Shoreline Mobility in Response to Changing Fluvial Sediment Supply. *Mar. Geology* 417, 106038. doi:10.1016/j.margeo.2019.106038

Baronas, J. J., Stevenson, E. I., Hackney, C. R., Darby, S. E., Bickle, M. J., Hilton, R. G., et al. (2020). Integrating Suspended Sediment Flux in Large Alluvial River Channels: Application of a Synoptic Rouse-Based Model to the Irrawaddy and Salween Rivers. *J. Geophys. Res. Earth Surf.* 125 (9), e2020JF005554. doi:10.1029/2020JF005554

Bird, M. I., Robinson, R. A. J., Win Oo, N., Maung Aye, M., Lu, X. X., Higgitt, D. L., et al. (2008). A Preliminary Estimate of Organic Carbon Transport by the Ayeyarwady (Irrawaddy) and Thanlwin (Salween) Rivers of Myanmar. *Quat. Int.* 186 (1), 113–122. doi:10.1016/j.quaint.2007.08.003

Choi, K., Kim, D., and Jo, J. (2020). Morphodynamic Evolution of the Macrotidal Sittaung River Estuary, Myanmar: Tidal versus Seasonal Controls. *Mar. Geology* 430, 106367. doi:10.1016/j.margeo.2020.106367

Egbert, G. D., and Erofeeva, S. Y. (2002). Efficient Inverse Modeling of Barotropic Ocean Tides. *J. Atmos. Oceanic Technol.* 19 (2), 183–204. doi:10.1175/1520-0426(2002)019<0183:eimobo>2.0.co;2

Environmental Modeling Center (2003). *The GFS Atmospheric Model.* College Park, MD: National Centers for Environmental Prediction Office. Note 442, 14.

Flynn, E. R., Kuehl, S. A., Harris, C. K., and Fair, M. J. (in press). Sediment and Terrestrial Organic Carbon Budgets for the Offshore Ayeyarwady Delta, Myanmar: Establishing a Baseline for Future Change. *Mar. Geology*. 106782. doi:10.1016/j.margeo.2022.106782

Friedrichs, C. T., Wright, L. D., Hepworth, D. A., and Kim, S. C. (2000). Bottom-Boundary-Layer Processes Associated with Fine Sediment Accumulation in Coastal Seas and Bays. *Continental Shelf Res.* 20 (7), 807–841. doi:10.1016/s0278-4343(00)00003-0

Glenn, S. M., and Grant, W. D. (1987). A Suspended Sediment Stratification Correction for Combined Wave and Current Flows. *J. Geophys. Res. Oceans* 92 (C8), 8244–8264.

Glover, H. E., Ogston, A. S., Fricke, A. T., Nittrouer, C. A., Aung, C., Naing, T., et al. (2021). Connecting Sediment Retention to Distributary – Channel Hydrodynamics and Sediment Dynamics in a Tide-dominated delta: The Ayeyarwady Delta, Myanmar. *J. Geophys. Res. Earth Surf.* 126 (3), e2020JF005882. doi:10.1029/2020jf005882

Grill, G., Lehner, B., Thieme, M., Geenen, B., Tickner, D., Antonelli, F., et al. (2019). Mapping the World's Free-Flowing Rivers. *Nature* 569 (7755), 215–221. doi:10.1038/s41586-019-1111-9

Hanebuth, T. J. J., Lantzsch, H., and Nizou, J. (2015). Mud Depocenters on Continental Shelves-Appearance, Initiation Times, and Growth Dynamics. *Geo-Mar Lett.* 35 (6), 487–503. doi:10.1007/s00367-015-0422-6

Holdaway, G. P., Thorne, P. D., Flatt, D., Jones, S. E., and Prandle, D. (1999). Comparison Between ADCP and Transmissometer Measurements of Suspended Sediment Concentration. *Continental Shelf Res.* 19 (3), 421–441. doi:10.1016/s0278-4343(98)00097-1

Hossain, M. S., Sarker, S., Sharifuzzaman, S. M., and Chowdhury, S. R. (2020). Primary Productivity Connects Hilsa Fishery in the Bay of Bengal. *Sci. Rep.* 10 (1), 5659–5716. doi:10.1038/s41598-020-62616-5

Kuehl, S. A., Williams, J., Liu, J. P., Harris, C., Aung, D. W., Tarpley, D., et al. (2019). Sediment Dispersal and Accumulation Off the Ayeyarwady Delta–Tectonic and

Oceanographic Controls. *Mar. Geology* 417, 106000. doi:10.1016/j.margeo.2019.106000

Kuehl, S. A., Yang, S., Yu, F., Copard, Y., Liu, J., Nittrouer, C. A., et al. (2020). Asia's Mega Rivers: Common Source. Diverse Fates. *Eos Trans. Am. Geophys. Union* 101. doi:10.1029/2020EO143936

Liu, J. P., Kuehl, S. A., Pierce, A. C., Williams, J., Blair, N. E., Harris, C., et al. (2020). Fate of Ayeyarwady and Thanlwin Rivers Sediments in the Andaman Sea and Bay of Bengal. *Mar. Geology* 423, 106137. doi:10.1016/j.margeo.2020.106137

Matamin, A. R., Ahmad, F., Mamat, M., Abdullah, K., and Harun, S. (2015). Remote Sensing of Suspended Sediment Over Gulf of Martaban. *Ekologia* 34 (No. 1), 54–64. doi:10.1515/eko-2015-0006

McKee, B. A., Aller, R. C., Allison, M. A., Bianchi, T. S., and Kineke, G. C. (2004). Transport and Transformation of Dissolved and Particulate Materials on Continental Margins Influenced by Major Rivers: Benthic Boundary Layer and Seabed Processes. *Continental Shelf Res.* 24 (7-8), 899–926. doi:10.1016/j.csr.2004.02.009

Meade, R. H. (1996). "River-Sediment Inputs to Major Deltas," in *Sea-Level Rise and Coastal Subsidence* (Dordrecht: Springer), 63–85. doi:10.1007/978-94-015-8719-8_4

Milliman, J. D., and Farnsworth, K. L. (2013). *River Discharge to the Coastal Ocean: A Global Synthesis*. Cambridge, United Kingdom: Cambridge University Press.

Milliman, J. D., and Meade, R. H. (1983). World-Wide Delivery of River Sediment to the Oceans. *J. Geology* 91 (1), 1–21. doi:10.1086/628741

NASA Worldview Application (2021). Part of the NASA Earth Observing System Data and Information System (EOSDIS). Available at: https://worldview.earthdata.nasa.gov.

Ramaswamy, V., and Rao, P. S. (2014). Chapter 17 the Myanmar Continental Shelf. *Geol. Soc. Lond. Mem.* 41 (1), 231–240. doi:10.1144/M41.17

Ramaswamy, V., Rao, P. S., Rao, K. H., Thwin, S., Rao, N. S., and Raiker, V. (2004). Tidal Influence on Suspended Sediment Distribution and Dispersal in the Northern Andaman Sea and Gulf of Martaban. *Mar. Geology* 208 (1), 33–42. doi:10.1016/j.margeo.2004.04.019

Rao, P. S., Ramaswamy, V., and Thwin, S. (2005). Sediment Texture, Distribution and Transport on the Ayeyarwady Continental Shelf, Andaman Sea. *Mar. Geology* 216 (4), 239–247. doi:10.1016/j.margeo.2005.02.016

Rodolfo, K. S. (1969). Sediments of the Andaman Basin, Northeastern Indian Ocean. *Mar. Geology* 7 (5), 371–402. doi:10.1016/0025-3227(69)90014-0

Rodolfo, K. S. (1975). "The Irrawaddy Delta: Tertiary Setting and Modern Offshore Sedimentation," in *Deltas: Models for Exploration* (United States: Houston Geological Society), 329–348.

Scully, M. E., and Friedrichs, C. T. (2007). Sediment Pumping by Tidal Asymmetry in a Partially Mixed Estuary. *J. Geophys. Res. Oceans* 112 (C7), C07028. doi:10.1029/2006jc003784

Simpson, J. H., Brown, J., Matthews, J., and Allen, G. (1990). Tidal Straining, Density Currents, and Stirring in the Control of Estuarine Stratification. *Estuaries* 13 (2), 125–132. doi:10.2307/1351581

Smith, J. D., and McLean, S. R. (1977). Spatially Averaged Flow Over a Wavy Surface. *J. Geophys. Res.* 82 (12), 1735–1746.

Trowbridge, J. H., and Kineke, G. C. (1994). Structure and Dynamics of Fluid Muds on the Amazon Continental Shelf. *J. Geophys. Res.* 99 (C1), 865–874. doi:10.1029/93jc02860

Wang, X. H., and Wang, H. (2010). Tidal Straining Effect on the Suspended Sediment Transport in the Huanghe (Yellow River) Estuary, China. *Ocean Dyn.* 60 (5), 1273–1283. doi:10.1007/s10236-010-0298-y

Conflict of Interest: JC was employed by Blue Coast Engineering.

The remaining authors declare that the research was conducted in the absence of any commercial or financial relationships that could be construed as a potential conflict of interest.